

Article

Mycobacterium Bovis Strain Ravenel is Attenuated in Cattle

Syeda A. Hadi¹*, Evan P. Brenner¹*, Mitchell V. Palmer², W. Ray Waters², Tyler C. Thacker³, Catherine Vilchèze⁴, Michelle H. Larsen⁴, William R. Jacobs, Jr.⁴ and Srinand Sreevatsan¹*

¹ Pathobiology and Diagnostic Investigation Department, Michigan State University, East Lansing, MI

² National Animal Disease Center, Agricultural Research Service, US Department of Agriculture, Ames, IA

³ National Veterinary Services Laboratories, US Department of Agriculture, Ames, IA

⁴ Howard Hughes Medical Institute and Department of Microbiology and Immunology, Albert Einstein College of Medicine, Bronx, NY

⁵ Authors contributed equally to the manuscript.

* Correspondence: S. Sreevatsan, 784 Wilson Road, College of Veterinary Medicine, East Lansing, MI 48824; E-mail: sreevats@msu.edu

Abstract: *Mycobacterium tuberculosis* variant *bovis* (MBO) has one of the widest known mammalian host ranges, including humans. Despite characterization of this pathogen in the 1800s, and whole genome sequencing of a UK strain (AF2122) nearly two decades ago, the basis of its host specificity and pathogenicity remains poorly understood. Recent experimental calf infection studies show that MBO strain Ravenel (MBO Ravenel) is attenuated in the cattle host. In the present study, experimental infections were performed to define attenuation and whole genome sequencing completed to identify regions of differences (RD) and single nucleotide polymorphisms (SNPs) to explain the observed attenuation. Comparative genomic analysis of MBO Ravenel against three pathogenic strains of MBO (strains AF2122-97, 10-7428 and 95-1315) was performed. Experimental infection studies on 5 calves each, with either MBO Ravenel or 95-1315, revealed no visible lesions in all 5 animals in the Ravenel group despite robust IFN- γ responses. Out of 486 polymorphisms in the present analysis, 173 were unique to MBO Ravenel among the strains compared. A high-confidence subset of 9 unique SNPs were missense mutations in genes with annotated functions impacting 2 major MBO survival and virulence pathways: 1) Cell wall synthesis & transport [*espH* (A103T), *mmpL8* (V888I), *aftB* (H484Y), *eccC5* (T507M), *rpfB* (E263G)], and 2) Lipid metabolism & respiration [*mycP1*(T125I), *pks5* (G455S), *fadD29* (N231S), *fadE29* (V360G)]. These substitutions likely contribute to the observed attenuation. Results from experimental calf infections and the functional attributions of polymorphic loci on the genome of MBO Ravenel provide new insights into the strain's genotype-disease phenotype associations.

Keywords: bovine tuberculosis; TB; attenuation; genomes; immunopathogenesis; SNPs

1. Introduction

Mycobacterium tuberculosis variant *bovis* (*Mycobacterium bovis* or MBO) causes significant economic hardship for livestock producers. *M. bovis*, a member of the *Mycobacterium tuberculosis* complex, is infectious to humans [1,2] and causes ~150,000 cases of human disease every year [3]. The overall virulence of MBO is generally greater than that of *M. tuberculosis* [4-7].

Historically, inoculation of rabbits was used to discriminate *M. tuberculosis* variant *tuberculosis* (MTB) from MBO within clinical samples; rabbits are typically resistant to MTB but highly susceptible to MBO infection. In contrast, guinea pigs and mice are susceptible to both MTB and MBO.

The MBO type strain for many comparative pathogenesis studies is *M. bovis* Ravenel (ATCC strain 35720). The Ravenel strain was isolated from a tuberculous cow circa 1900 and deposited in the Trudeau Mycobacterial Culture Collection in 1910. At the Trudeau Institute, this strain was used for pathogenesis and virulence studies in mice, rabbits, and guinea pigs.

MBO strain Ravenel has been used in diagnostic [8], immunopathogenesis [5,6], chemotherapy [9], and vaccine efficacy studies [10,11]. Current stocks of MBO Ravenel (ATCC strain 35720) are fully virulent in rabbits [12,13], guinea pigs [13], and mice [13-15] but attenuated in cattle.

Experimental infection of calves with MBO strains such as 95-1315 at the National Animal Disease Center (NADC) in the US [16], WAg202 at AgResearch in New Zealand [17], and AF2122/97 at Animal Health and Veterinary Laboratory Agency (AHVLA) in the United Kingdom [18,19] consistently result in progressive disease in cattle including typical granulomatous gross and microscopic lesions with recovery of bacilli from affected tissues. However, in a bovine TB vaccine efficacy study with cattle by Khare et al., 2007 [11], gross tuberculous lesions were not detected in vaccinated or unvaccinated groups upon necropsy 160 days after intranasal delivery of 10^6 colony forming units (CFU) MBO Ravenel challenge despite recovery of MBO Ravenel from 10/10 unvaccinated and 4/10 vaccinated animals. The authors concluded that experimental MBO Ravenel infection of cattle results in sub-clinical disease. Because of this deficiency, pathogenesis studies no longer employ MBO Ravenel. Given these reports on apparent disease phenotype variations among different strains of MBO, the objectives of the present study were: (1) to compare the virulence of MBO Ravenel to MBO strain 95-1315 in cattle and (2) compare the genome sequences of MBO Ravenel to three virulent strains of MBO.

2. Methods

2.1. *Mycobacterium tuberculosis* variant *bovis* challenge strains

Two strains of MBO were used for challenge inoculum: (1) MBO strain 95-1315 [USDA, Animal Plant and Health Inspection Service (APHIS) designation] originally isolated from a white-tailed deer in Michigan, USA(20) and (2) MBO strain Ravenel (ATCC 35720) obtained from John Chan at Albert Einstein College of Medicine, Bronx, NY and freezer stocks were kept at NADC. Strains were prepared using standard procedures [20] in Middlebrook 7H9 liquid media (Becton Dickinson, Franklin Lakes, NJ) supplemented with 10% oleic acid-albumin-dextrose complex (OADC) plus 0.05% Tween 80 and 0.5% Glycerol (strain Ravenel only).

2.2. Cattle studies: treatment groups and aerosol MBO challenge procedures

Holstein steers (n=18, ~1yr of age) were obtained from a TB-free herd in Sioux Center, IA and housed in a biosafety level-3 (BSL-3) facility at the NADC, Ames, IA according to Institutional Biosafety and Animal Care and Use Committee guidelines. In an initial study, steers (n=3) received 10^5 CFU MBO Ravenel by aerosol. Briefly, inoculum ($\sim 10^5$ CFU) was delivered to restrained calves by nebulization into a mask (Trudell Medical International, London, ON, Canada) covering the nostrils and mouth. Inoculum was inhaled through a one-way valve into the mask and directly into the lungs via the nostrils. The process continued until the inoculum, a 1mL PBS wash of the inoculum tube, and an additional 2mL PBS were delivered, a process taking ~10 min. Strict BSL-3 safety protocols were followed to protect personnel from exposure to MBO.

In a follow-up study, treatment groups consisted of uninfected steers (n=5) and steers receiving either 10^5 CFU MBO strain 95-1315 (n=5) or 10^5 CFU MBO strain Ravenel (n=5) by aerosol [16].

All calves were euthanized ~3.5 months after challenge by intravenous administration of sodium pentobarbital. Tissues were examined for gross lesions and collected and processed for microscopic analysis and isolation of MBO. Tissues collected included: palatine tonsil; lung; liver; and mandibular, parotid, medial retropharyngeal, mediastinal, tracheobronchial, hepatic, and mesenteric lymph nodes. Lymph nodes were sectioned at 0.5cm intervals and examined. Each lung lobe was sectioned at 0.5 – 1.0cm intervals and examined separately. Lungs and lymph nodes (mediastinal and tracheobronchial) were evaluated using a semi-quantitative gross pathology scoring system adapted from

Vordermeier et al., 2002 [17]. Lung lobes (left cranial, left caudal, right cranial, right caudal, middle, and accessory) were individually scored based upon the following scoring system: 0 = no visible lesions; 1 = no external gross lesions, but lesions seen upon slicing; 2 = <5 gross lesions of <10mm in diameter; 3 = >5 gross lesions of <10mm in diameter; 4 = >1 distinct gross lesion of >10mm in diameter; 5 = gross coalescing lesions. Cumulative mean scores were then calculated for each entire lung. Lymph node pathology was based on the following scoring system: 0 = no necrosis or visible lesions; 1 = small focus (1 to 2mm in diameter); 2 = several small foci; 3 = extensive necrosis. Gross pathology data are presented as mean (\pm standard error) disease score for mediastinal lymph node, tracheobronchial lymph node, and lung.

Tissues collected for microscopic analysis were fixed by immersion in 10% neutral buffered formalin. For microscopic examination, formalin-fixed tissues were processed by standard paraffin-embedment techniques, cut in 5 μ m sections and stained with hematoxylin and eosin (H&E). Adjacent sections from sections containing caseous necrotic granulomata suggestive of tuberculosis were cut and stained by the Ziehl-Neelsen technique for visualization of acid-fast bacteria (AFB). Microscopic tuberculous lesions were staged (I-IV) as described by Wangoo [21]. Data are presented as total and mean number of granulomas observed in each histologic lesion stage (i.e., I – IV) for lung and mediastinal lymph node sections.

For quantitative assessment of mycobacterial burden, left tracheobronchial lymph nodes were removed, examined for gross lesions, weighed, and the entire lymph node (other than a small ~1g section for histology and qualitative culture) homogenized in phenol red nutrient broth using a blender (Oster, Shelton, CT). Logarithmic dilutions (10^0 - 10^{-9}) of homogenates in PBS were plated in 100 μ L aliquots plated on Middlebrook 7H11 selective agar plates (Becton Dickinson) and incubated for 8 weeks at 37°C [22]. Data are presented as mean (\pm standard error) CFU per gram of tissue.

2.3. IFN- γ whole blood assays.

Duplicate 250 μ L heparinized whole blood aliquots were distributed in 96-well plates with MBO purified-protein derivates (PPD) (10 μ g/mL, Prionics Ag, Schlieren, Switzerland), rESAT-6/CFP10 (1 μ g/mL), or no antigen (nil) and incubated at 39°C/5% CO₂ for 20 hours. IFN- γ concentrations in stimulated plasma were determined using a commercial ELISA-based kit (Bovigam™, Prionics Ag). Absorbance values of standards (recombinant bovine IFN- γ ; Endogen, Rockford, IL) and test samples were read at 450nm using an ELISA plate reader (Molecular Devices, Menlo Park, Calif.). Duplicate samples for individual treatments were analyzed and data presented as optical densities at 450nm of the response to MBO PPD minus the response to no-antigen (mean \pm SEM).

2.4. Delayed type hypersensitivity (DTH) responses (skin test procedures)

Fifteen days prior to necropsy, calves received 0.1mL (100 μ g) of MBO PPD and 0.1mL (40 μ g) of *Mycobacterium avium* PPD injected intradermally at separate clipped sites in the mid-cervical region according to guidelines described in USDA, Animal and Plant Health Inspection Service (APHIS), Veterinary Services (VS) circular 91-45-01 (APHIS, 2005) for the comparative cervical test. Skin thickness was measured with calipers prior to PPD administration and 72hrs after injection. A scattergram for interpretation of CCT results provided by USDA, APHIS, VS was used to categorize animals as negative, suspect or reactors. Balanced PPDs were obtained from the Brucella and Mycobacterial Reagents section of National Veterinary Services Laboratory, Ames, IA.

2.5. Whole genome sequencing of MBO Ravenel

MBO Ravenel was obtained from freezer stocks stored at NADC (APHIS, USDA) and cultured on Middlebrook 7H10 slants (Hardy Diagnostics, Santa Maria, CA) for 14 days. Colonies were harvested for DNA extraction. Paired-end (2 x 150bp) library preparation

was followed by NovaSeq Illumina genome sequencing (Novogene). All reads were quality-checked, and adapters trimmed by Novogene's in-house custom software (v1.0). Sequences were then checked for contamination using Kraken 2 with default parameters and the author-provided "Standard" database (24). All reads were used to assemble the genome *de novo* irrespective of Kraken's taxonomy assignment. ABySS v2.1.5 (k-value=96) was used to assemble the genome (25). RagTag v1.1.0 was used to perform MBO AF2122/97 (GenBank accession number [LT708304](#)) reference-based assembly correction followed by scaffolding [23]. QCAST v5.0.2 was used to analyze scaffolds [24], and generate Circos plots [25] and Icarus views (*Ravenel-Supplementary material2-Circos-Images*). Uninformative contigs (<200 bp) were removed before submission to the Prokaryotic Genome Annotation Pipeline (PGAP) v5.1 [26]. The draft genome was submitted to both PATRIC [27] and NCBI.

2.6. Genome comparisons

2.6.1. Identification of single nucleotide polymorphisms (SNPs) in MBO Ravenel

MBO Ravenel's genomic comparisons were performed against the reference strain MBO AF2122/97, MBO 95-1315 (isolated from deer, PATRIC ID [1765.15](#)) and MBO 10-7428 (isolated from cattle). MBO 10-7428 was submitted to Novogene for resequencing as described above, assembled as a draft genome (PATRIC ID [1765.618](#); GenBank: [JA-GEUC000000000.1](#)), and used for comparative genomics and SNP extraction. Snippy [28] was used to call SNPs from MBO Ravenel, MBO 10-7428 and MBO 95-1315 using MBO AF2122/97 as the reference. The snippy-core script was used to extract SNPs at all positions with sufficient coverage for base calling from all four genomes, and SNPs not unique to MBO Ravenel were removed from the analysis. The SNPs that remained at this stage were unique to MBO Ravenel. Among these, only the missense mutations in genes with a putative function assigned were crosschecked against the annotated genome on PATRIC.

2.6.2. Region of difference (RD) analysis

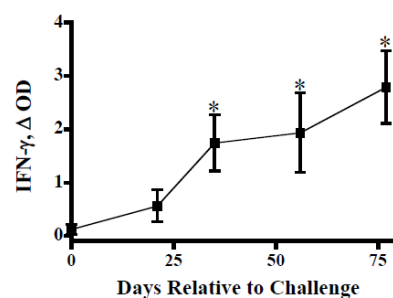
RD-Analyzer [29] was used to identify *in silico* regions of difference for MBO Ravenel when compared against MBO AF2122/97 using raw reads of the available genome.

3. Results

3.1. Experimental infection of cattle

In an initial study with cattle (n=3), aerosol MBO Ravenel ($\sim 10^5$ CFU) elicited immune responses (i.e., DTH and IFN- γ) to MBO antigens (Figure 1); yet, 2.5 months after challenge, tuberculous lesions were not detectable in two animals and a single small granuloma was detected in the lung of the third animal. The low virulence of this strain in cattle was surprising given the high virulence of MBO Ravenel in mice, rabbits, and guinea pigs [7,13,14].

A. IFN- γ Response



B. DTH Responses

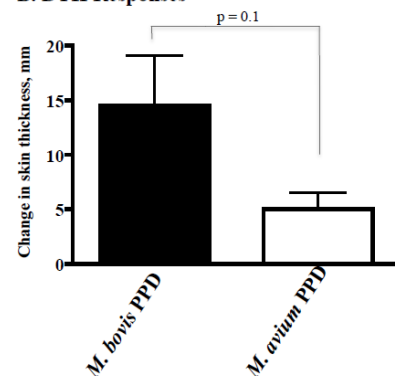


Figure 1. Interferon- γ (panel A) and delayed type hypersensitivity (DTH, panel B) responses upon aerosol *M. bovis* Ravenel (n = 3) infection. *Panel A.* Whole blood cultures were stimulated with 20 mg/ml *M. bovis* PPD (Prionics AG) or medium alone (no stimulation) for 48 hrs. Stimulated plasma were harvested and IFN- γ concentrations determined by ELISA (Bovigam, Prionics, Ag). Values represent mean (\pm standard error) responses to antigen minus the response to media alone (D OD) for *M. bovis* Ravenel-infected cattle. Response kinetics to rESAT-6/CFP10 were similar to *M. bovis* PPD responses (data not shown). * Differs ($p < 0.05$) from pre-challenge (Day 0) responses. *Panel B.* Approximately 2 months after challenge, 0.1 ml (100 mg) of *M. bovis* PPD and 0.1 ml (40 mg) of *M. avium* PPD were injected intradermally at separate clipped sites in the mid-cervical region of each calf. Values represent mean (\pm standard error) change in skin thickness (i.e., 72 hrs post injection minus pre-injection).

To confirm this finding, an immunopathogenesis study was performed to directly compare the virulence of MBO strain Ravenel (n=5) to that of MBO strain 95-1315 (n=5), a strain of consistent virulence in cattle (15, 16). Significant IFN- γ responses to rESAT-6/CFP10 (E:C) or MBO PPD were elicited by MBO infection (Figure 2), regardless of strain. IFN- γ responses did not differ ($p > 0.05$) between the two challenge groups. Significant DTH responses to PPD's were also elicited by MBO infection (Figure 3). Responses to MBO PPD by MBO 95-1315 infected calves exceeded ($p < 0.05$) respective responses by MBO Ravenel infected calves.

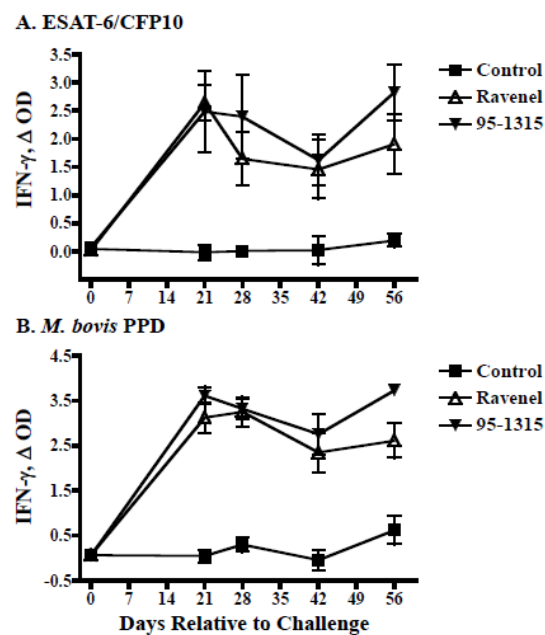


Figure 2. Interferon- γ responses upon *M. bovis* infection of cattle. Whole blood cultures were stimulated with 1 mg/ml rESAT-6:CFP-10 (panel A), 20 mg/ml *M. bovis* PPD (panel B), or medium alone (no stimulation) at 39°C / 5% CO₂ for 20 hrs. Stimulated plasma were harvested and IFN- γ concentrations determined by ELISA (Bovigam, Prionics, Ag). Values represent mean (\pm standard error) responses to antigen minus the response to media alone (D OD) for non-infected cattle (controls, closed squares) or cattle infected with *M. bovis* strain Ravenel (open triangles) or strain 95-1315 (closed inverted triangles). All responses elicited after challenge with *M. bovis* (either strain) exceeded ($p < 0.05$) respective responses in non-infected (control) cattle. Responses elicited by *M. bovis* Ravenel infection did not differ ($p > 0.05$) from responses elicited by *M. bovis* 95-1315.

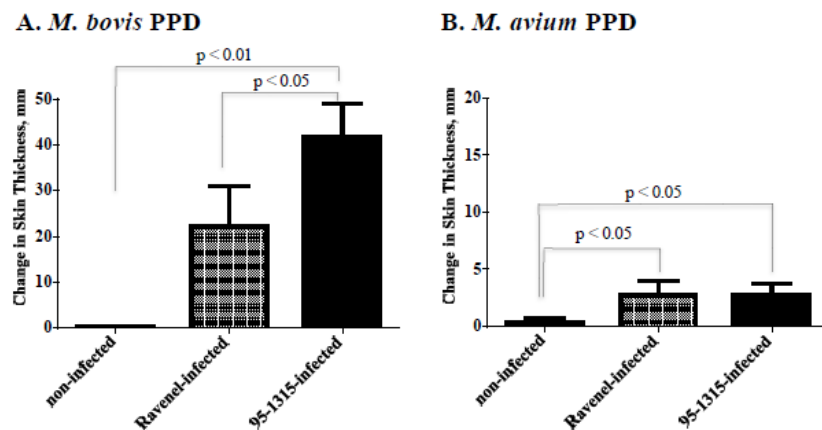


Figure 3. Delayed type hypersensitivity responses upon aerosol *M. bovis* infection. Approximately 3.25 months after challenge, 0.1 ml (100 mg) of *M. bovis* PPD and 0.1 ml (40 mg) of *M. avium* PPD were injected intradermally at separate clipped sites in the mid-cervical region of each calf according to USDA, APHIS uniform methods (APHIS 91-45-011). Values represent mean (\pm standard error) change in skin thickness (i.e., 72 hrs post injection minus pre-injection). Differences between treatment groups are indicated on each graph.

Despite robust cell-mediated immune (CMI) responses, gross tuberculous lesions were not detectable in 4/5 MBO Ravenel-infected cattle (**Error! Reference source not found.**). As with the initial study, one MBO Ravenel-infected steer had a single small granuloma in the left caudal lung lobe. In contrast, all 5 MBO 95-1315-infected cattle had granulomatous lesions in lungs and lung-associated lymph nodes.

Table 1. Cattle Infection Study, Gross Pathology Results.

| Treatment Group | Mean Disease Score ^a | | |
|-----------------------------|---------------------------------|----------------------------|----------------------------|
| | Tracheobronchial lymph nodes | Mediastinal lymph nodes | Lung |
| Non-infected | 0 \pm 0 (0 / 5) | 0 \pm 0 (0 / 5) | 0 \pm 0 (0 / 5) |
| MBO strain Ravenel infected | 0 \pm 0 (0 / 5) | 0 \pm 0 (0 / 5) | 0.04 \pm 0.04 (1 / 5) |
| MBO strain 95-1315 infected | 1.4 \pm 0.2 * (5 / 5) | 1.4 \pm 0.2 * (5 / 5) | 1.2 \pm 0.3 * (5 / 5) |

^aAt necropsy, tracheobronchial lymph nodes, mediastinal lymph nodes, and lungs were evaluated for lesions based upon a scoring system adapted from Vordermeier et al., 2002. Mean disease scores are presented as mean \pm sem. In addition, the # of animals with lesions / # of animals per group is provided in parentheses under disease scores. * Differs ($p < 0.05$) from other treatment groups relative to tissue.

In contrast to gross and microscopic pathology findings, MBO Ravenel was isolated from tissues of 4/5 cattle (**Error! Reference source not found.**). Tracheobronchial lymph nodes were the most common site for detectable MBO Ravenel colonization, despite no observable gross lesions in the tracheobronchial lymph nodes. As expected from prior studies, MBO 95-1315 was isolated from lungs and lung-associated lymph nodes from all 5 calves receiving this strain. Mean colonization of tracheobronchial lymph nodes in MBO 95-1315-infected calves exceeded that of MBO Ravenel-infected calves.

Table 2. Cattle Infection Study, Recovery of *M. bovis* from lesions.

| Treatment Group | Quantitative Culture (CFU/g) ^a | Qualitative Culture ^b | | |
|----------------------|---|----------------------------------|------------------------|-------|
| | | Tracheobronchial Lymph Node | Mediastinal Lymph Node | Lung |
| Non-infected | 0 ± 0 | 0 / 5 | 0 / 5 | 0 / 5 |
| MBO Ravenel infected | 427 ± 1246 | 4 / 5 | 1 / 5 | 0 / 5 |
| MBO 95-1315 infected | 28,141 ± 9063 * | 5 / 5 | 4 / 5 | 3 / 5 |

^aTo eliminate bias based on organ sampling site, entire tracheobronchial lymph nodes (other than a small ~1 gram section for histology and qualitative culture) were homogenized and cultured for *M. bovis*. Values represent mean (± standard error) CFU / g of tissue. *Differs from non- and *M. bovis* Ravenel-infected groups, $p < 0.05$. ^bFor qualitative culture, values represent the number of tissues in which *M. bovis* was isolated / number of animals per group.

3.2. Whole genome sequencing

The MBO Ravenel genome has been assembled and deposited in publicly accessible databases (GenBank: [JAGEUB000000000.1](https://www.ncbi.nlm.nih.gov/nuclink/JAGEUB000000000.1); PATRIC: [1765.617](https://patric.brc.utk.edu/1765.617)). The sequencing yielded 9,074,522 spots (2x150bp/spot). Draft assembly of the genome after removal of uninformative contigs (<200bp) yielded 18 final contigs. Total length of the genome was 4,377,551bp with a GC percentage of 65.6%. Length of the longest contig (N50) was 4,371,545bp with a coverage of 625.8x. The NCBI-based Prokaryotic Genome Annotation Pipeline (PGAP) identified 4,058 coding sequences (CDSs), 3 rRNAs, 45 tRNAs, 3 noncoding RNAs, and 192 pseudogenes.

3.3. Genome comparisons

3.4. SNPs from MBO Ravenel versus virulent MBO strains

Comparisons between strains AF2122/97, 10-7428, Ravenel, and 95-1315 revealed no large-scale deletions in the Ravenel genome compared to the AF2122/97 genome. A total of 974 single nucleotide polymorphisms (SNPs) were extracted from the three strains against the AF2122/97 reference. Out of 974 SNPs in the set, 173 were present in and unique to MBO Ravenel. Of these, 95 were missense, and 54/95 missense mutations were in genes with a putative function assigned. Regions of the genome assembly flagged by QUAST as having potential for any degree of misassembly were excluded, leaving a subset of 32 highest-confidence SNPs (Figure 4, Figure 5, and Ravenel Supplementary table). Nine highest-confidence SNPs were within “specialty genes” in the functionally annotated genome available on PATRIC ([1765.617](https://patric.brc.utk.edu/1765.617)). These nine SNPs were cross-checked in Mycobrowser for their functional categorization (**Error! Reference source not found.**) [30]. Two functional categories were identified: (i) cell wall and cell processes (*espH*, *mmpL8*, *aftB*, *eccC5*, *rpfB*), and (ii) respiration or lipid metabolism (*mycP1*, *pks5*, *fadD29*, *fadE29*).

Table 3. Nine MBO Ravenel-specific single nucleotide polymorphisms (SNPs) hypothesized to contribute to attenuation of MBO Ravenel. High-confidence missense SNPs were extracted from MBO strain Ravenel (strain AF2122/97 as reference) and compared to strains 10-7428 and 95-1315. (74).

| Position | Gene Name | Gene Identifier | Mycobrowser Classification | Functional Annotation | DNA change (Protein change) |
|----------|--------------|-----------------|---|---|-----------------------------|
| 4305161 | <i>mycP1</i> | MB3913C | Intermediary metabolism and respiration | membrane-anchored mycosin mycp1 (serine protease) (subtilisin-like protease) (subtilase-like) (mycosin-1) | C374T (T125I) |

| | | | | | |
|---------|---------------|---------|------------------------------|--|----------------|
| 4283808 | <i>espH</i> | MB3897 | Cell wall and cell processes | esx-1 secretion-associated protein | G307A (A103T) |
| 4229553 | <i>mmpL8</i> | MB3853C | Cell wall and cell processes | conserved integral membrane transport protein | G2662A (V888I) |
| 4208072 | <i>aftB</i> | MB3835C | Cell wall and cell processes | possible arabinofuranosyltransferase | C1450T (H484Y) |
| 2015643 | <i>eccC5</i> | MB1812 | Cell wall and cell processes | esx conserved component ecc5. esx-5 type vii secretion system protein | C1520T (T507M) |
| 1129357 | <i>rpfB</i> | MB1036 | Cell wall and cell processes | Probable resuscitation-promoting factor | A788G (E263G) |
| 1715469 | <i>pks5</i> | MB1554C | Lipid metabolism | Probable polyketide synthase | G1363A (G455S) |
| 3262864 | <i>fadD29</i> | MB2974C | Lipid metabolism | fatty-acid-amp ligase fadD29 (fatty-acid-amp synthetase) (fatty-acid-amp synthase) | A692G (N231S) |
| 3929690 | <i>fadE29</i> | MB3573C | Lipid metabolism | Probable Acyl-CoA dehydrogenase | T1079G (V360G) |

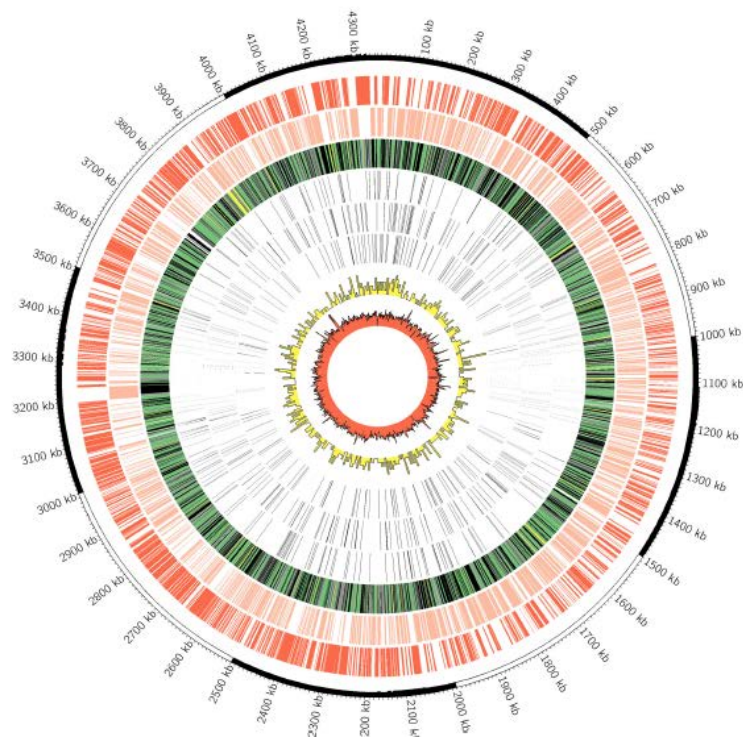


Figure 4. Genome-wide comparisons of Ravenel and 95-1315. The outermost circle is scale in kilobase pairs. The 1st two rings depict coding regions in the positive and negative strands, respectively. The 3rd ring depicts predicted subcellular localization of each protein, with blue = cell wall, green = cytoplasmic, black = cytoplasmic membrane, yellow = extracellular, and grey = unknown. Rings 4-6 depicts SNPs that are shared by both strains Ravenel and 95-1315 (Ring 4), unique to strain 95-1315 (Ring 5), and unique to strain Ravenel (Ring 6). Ring 7 in yellow depicts SNP density across the *M. bovis* genome in 10-kb increments. Ring 8 in red depicts G+C content in a 3-kb sliding window.

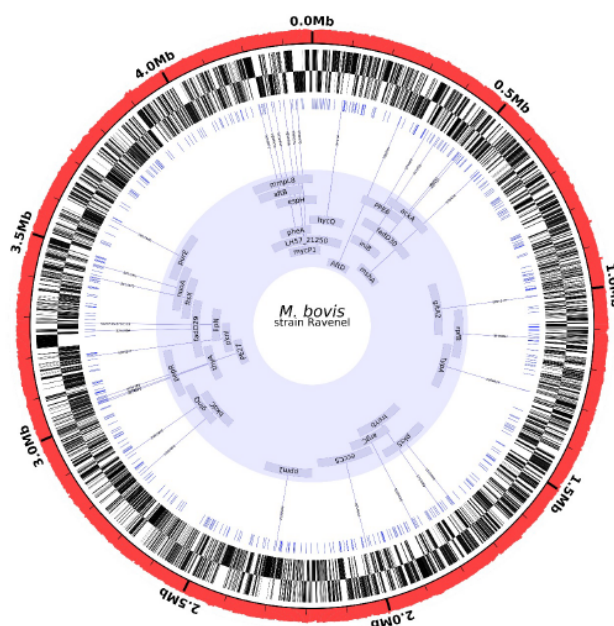


Figure 5. Position of 32 high-confidence missense polymorphisms in the Ravenel assembly. The Ravenel genome assembly (GCA_018305025.1) was downloaded and contigs longer than 1000bp were visualized using Circlearator (69). Working inwards, the rings represent: red, genome %GC; black, genes-fw; black, genes-rev; blue, total unique polymorphisms (n=486); blue central ring with labeled loci, 32 high-confidence missense polymorphisms in genes with annotated function. Of these polymorphisms, 31 are SNPs, and 1 is a multi-nucleotide polymorphism (lipN). Nine SNPs in this innermost subset are discussed in greater detail in the manuscript.

Region of difference (RD) analysis of MBO Ravenel revealed that RD9, RD4, RD7, RD8, RD10, RD11 and RD12 were absent (classic MBO type).

4. Discussion

Experimental and clinical studies show that MBO Ravenel is attenuated and elicits a robust immune response in cattle. Genome-wide SNPs studies in *M. tuberculosis* have been shown to have sufficient resolution to develop trait-allele interactions. In the present study, we hypothesized that drivers of attenuation are enciphered in the genome of MBO Ravenel (11) and performed comparative genomic analysis of Ravenel against 3 clinical MBO strains – 95-1315, 10-7428, and AF2122/97. Disease phenotype was assessed by experimental infections with either Ravenel or 95-1315.

The present study utilized genomes of these select clinical strains to draw comparisons against the attenuated strain MBO Ravenel. This led to identification of 32 highest confidence MBO Ravenel-specific non-synonymous SNPs, visualized by affected locus and position across the genome in Figure 5. Among these, a subset of 9 SNPs was selected based on functional annotation of impacted loci. These SNPs may contribute to reduced virulence and an attenuated phenotype as they affect cell wall synthesis-and transport-associated genes, pathways critical for the metabolism and intracellular survival of the pathogen.

4.1. Ravenel elicits robust cell mediated immune response but is attenuated

Experimental calf infection with Ravenel or 95-1315 revealed that the former strain did not produce granulomata but was isolated from lymph nodes. The low virulence of this strain in cattle was surprising given the high virulence of *M. bovis* Ravenel in mice,

rabbits, and guinea pigs (7, 13, 14). Furthermore, comparative immunopathogenesis revealed significant IFN- γ responses to rESAT-6/CFP10 or *M. bovis* PPD were elicited by *M. bovis* infection, regardless of the strain used. These findings are consistent with the observations of Khare et al., (11) who demonstrated similar attenuation of Ravenel in a vaccination-challenge trial. Taken together, our findings confirm that Ravenel is attenuated in the bovine host deserving a deeper explanation for the observed phenotype.

4.2. Ravenel carries SNPs in genes encoding cell wall integrity

Members of the MTBC possess unique Type VII secretion systems (ESX systems). These secretion systems contribute to virulence (ESX-1, -3, -5), nutrient uptake (ESX-5), metal homeostasis (ESX-3), and export of PE/PPE family proteins (ESX-5)(34). Disruption of these systems is associated with attenuation [35]. In MBO Ravenel's ESX-5 system, we identified the polymorphism C1530T (T507M) in *eccC5*. The ATPase encoded by *eccC5* has 3 nucleotide binding domains hypothesized to be essential for substrate recognition (36). Ates et al., demonstrated that NBD mutations impaired bacterial growth [37]. The mutation in MBO Ravenel's *eccC5* (T507M) falls directly adjacent to NBD-1 (K506), which may destabilize binding and function of this virulence-associated system (37). MBO Ravenel also has mutation G307A (A103T) in *espH*, a gene associated with the ESX-1 virulence system [31].

The mycobacterial membrane protein [large] (*mmpL*) genes encode a broad family of transmembrane-transport proteins believed to be involved in fatty acid transportation by performing the function of flippases [32-35]. Essential for survival, members of this family like MmpL3 have been proposed as a druggable target [36], and research into small molecule inhibitors has yielded mycobactericidal compounds [31]. Williams et al., reported a list of mutations in the *mmpL3*-mutant strains of which none were identifiable in MBO Ravenel [31]. Instead MBO Ravenel had missense mutation G2662A (V888I) in *mmpL8*. Unlike *mmpL3*'s role in survival of mycobacteria, evidence is rather limited for *mmpL8* specifically. Nonetheless, being from the same family of proteins mutation in *mmpL8* might affect transportation of pathogenesis-associated compounds.

Biosynthesis of arabinogalactan by *aftB* is fundamental for the mycobacterial cell wall [37,38]. Raad et al. developed a *Corynebacterium glutamicum* Δ *aftB* mutant that caused outer membrane destabilization [38]. Jankute et al., demonstrated similar results in *M. smegmatis* [37]. Ravenel carries a mutation in *aftB* C1450T (H484Y) and whether this mutation results in deficient biosynthesis of arabinogalactan remains to be explored.

Encoded by *rpfB*, resuscitation promoting factor (RPF), in partnership with RPF-interacting [39-43]. The resuscitation promoting factor cleaves peptidoglycan, employing E292 in its catalytic pocket [44,45]. MBO Ravenel carries *rpfB* polymorphism A788G (E263G) that, while outside Squeglia et al.'s observed catalytic region [45], may conformationally affect the downstream pocket by replacement of a charged amino acid with a flexible glycine residue.-

4.3. Ravenel carries SNPs in genes associated with respiration or lipid metabolism

Lipids are the primary carbon source for mycobacteria [46-48]. The *fadD* and *fadE* families of genes are involved in long-chain fatty acid synthesis in mycobacteria, encoding ligase, synthetase and dehydrogenase. The enzyme encoded by *fadD29* converts long-chain fatty acids to the acyl adenylates required for phenol glycolipid (PGL) production, which in turn is required for the synthesis of outer membrane of MTB [49]. In the present study, MBO Ravenel carried a mutation in *fadD29* A692G (N231S). PGL synthesis is required for mycobacterial viability, so non-synonymous changes warrant scrutiny [49,50]. MTB relies on host cholesterol import for carbon supply and survival during chronic infection through *fadE29*. Knockout studies by Thomas et al., and Gilbert et al., determined that *fadE28* and *fadE29* are essential for degradation of cholesterol metabolites [51,52]. MBO Ravenel *fadE29* has missense mutation T1079G (V360G). The downstream effects of

non-synonymous mutations in both *fadE29* and *fadD29* may contribute to alterations in bacterial viability.

Polyketide synthase 5, encoded by *pks5*, has been identified as a virulence-associated biomarker of MTBC infection in cattle [53]. The product of *pks5* is thought to be involved in multimethyl-branched fatty acid synthesis required for lipooligosaccharide (LOS) biosynthesis [54]. Loss of *pks5* leads to severe MTB growth defects in animal models [55]. In MBO Ravenel, we observed a G1363A mutation (G455S) in *pks5*, though any effects on function require experimental testing.

The serine protease mycosin (MycP₁) is a conserved membrane component of ESX-1 and ESX-5 systems [56]. Ohol *et al.* (2010) found that the inhibition of MycP₁ protease activity leads to increased ESX-1 substrate secretion [57]. C374T (T125I) in *mycP1* is therefore another SNP of interest in MBO Ravenel, as destabilization of this protease is known to lead to dysregulation of the tightly controlled ESX-1 machinery. Considering the ESX-1-containing RD-1 is believed to be a major contributor to the substantial attenuation of MBO BCG [15,57-59], any disruption of this system by alternate means could explain virulence deficiencies despite RD-1's presence.

Out of 32 genes with functional annotations containing missense mutations unique to MBO Ravenel, nine involved in cell wall integrity and critical metabolism have been described here. A single mutation could not reasonably explain the experimental attenuation observed in MBO Ravenel when compared to fully virulent strains, though the cumulative effect of many SNPs across the genome may have contributed to impairment of pathogenesis. While only a subset of the observed SNPs have been discussed here, the remaining 23 MBO Ravenel-specific missense mutations, as well as those in loci without annotated function and those in intergenic regions likely also play some role.

5. Conclusion

Our aim was to compare the *in vivo* virulence of MBO Ravenel to MBO 95-1315 in the original bovine host, as well as discover the pathways impacted by mutations across the MBO Ravenel genome. Cattle infection experiments supported previously identified differences in MBO Ravenel pathology in the bovine host, and detection of robust immune responses across animals despite the absence of gross lesions supports the Ravenel strain's deficiency in pathogenesis, causing only subclinical infection in contrast to the observed virulence from MBO 95-1315. The set of identified high-confidence missense polymorphisms in key genes involved with survival and pathogenesis of MBO provides a realistic genetic basis for attenuation. Which, if any, of these changes lead to functional impacts still requires elucidation. In summary, we confirm MBO Ravenel is attenuated and presents sub clinically in the bovine host despite its broad genomic structural similarities to fully virulent MBO strains. A constellation of polymorphisms in key genes may instead explain its striking differences in disease phenotype when compared to virulent MBO 95-1315.

ACKNOWLEDGEMENTS – Research in the Sreevatsan lab is funded by USDA (2018-67015-28288) and start-up funds provided by College of Veterinary Medicine, Michigan State University. Syeda Anum Hadi was supported by Fulbright fellowship program. Animal studies were funded by the USDA, Current Research Information System (CRIS) #3625-32000-232-00.

References

1. Kleeberg, H.H. Human tuberculosis of bovine origin in relation to public health*. In *Rev. sci. tech. Off. int. Epiz.*, 1984; Vol. 3, pp 23-27.
2. Wilkins, M.J.; Meyerson, J.; Bartlett, P.C.; Spieldenner, S.L.; Berry, D.E.; Mosher, L.B.; Kaneene, J.B.; Robinson-dunn, B.; Stobierski, M.G.; Boulton, M.L. *Mycobacterium bovis* Infection and Bovine. 2008; Vol. 14, pp 657-660.
3. WHO. Global Tuberculosis Report. In *Geneva: World Health Organization*, 2018.

4. Dannenberg, A.M. Pathogenesis of pulmonary Mycobacterium bovis infection: basic principles established by the rabbit model. In *Tuberculosis*, 2001; Vol. 81, pp 87-96.
5. Dunn, P.L.; North, R.J. Virulence ranking of some Mycobacterium tuberculosis and Mycobacterium bovis strains according to their ability to multiply in the lungs, induce lung pathology, and cause mortality in mice. In *Infection and Immunity*, 1995; Vol. 63.
6. Henderson, H.J.; Dannenberg, A.M.; Lurie, M.B. Phagocytosis of Tubercle Bacilli By Rabbit Pulmonary Alveolar Macrophages and Its Relation To Native Resistance To Tuberculosis. In *Journal of immunology (Baltimore, Md. : 1950)*, 1963; Vol. 91.
7. Nedeltchev, G.G.; Raghunand, T.R.; Jassal, M.S.; Lun, S.; Cheng, Q.J.; Bishai, W.R. Extrapulmonary dissemination of mycobacterium bovis but not mycobacterium tuberculosis in a bronchoscopic rabbit model of cavitary tuberculosis. In *Infection and Immunity*, 2009; Vol. 77.
8. Harboe, M.; Nagai, S. MPB70, a unique antigen of Mycobacterium bovis BCG. In *American Review of Respiratory Disease*, 1984; Vol. 129.
9. Tsenova, L., Sokol, K., Freedman, V. H., & Kaplan, G. A Combination of Thalidomide Plus Antibiotics Protects Rabbits from Mycobacterial Meningitis-Associated Death. In *The Journal of Infectious Diseases*, 1998; Vol. 177, pp 1563-1572.
10. Kato K, Y.K., Okuyama H, Kimura T. Microbicidal activity and morphological characteristics of lung macrophages in Mycobacterium bovis BCG cell wall-induced lung granuloma in mice. In *Infect Immun.*, 1984; Vol. 45, pp 325-331.
11. Khare, S.; Hondalus, M.K.; Nunes, J.; Bloom, B.R.; Garry Adams, L. Mycobacterium bovis Δ leuD auxotroph-induced protective immunity against tissue colonization, burden and distribution in cattle intranasally challenged with Mycobacterium bovis Ravenel S. In *Vaccine*, 2007; Vol. 25, pp 1743-1755.
12. Converse, P.J.; Dannenberg, A.M.; Shigenaga, T.; McMurray, D.N.; Phalen, S.W.; Stanford, J.L.; Rook, G.A.W.; Koru-Sengul, T.; Abbey, H.; Estep, J.E., et al. Pulmonary bovine-type tuberculosis in rabbits: Bacillary virulence, inhaled dose effects, tuberculin sensitivity, and Mycobacterium vaccae immunotherapy. In *Clinical and Diagnostic Laboratory Immunology*, 1998; 10.1128/cdli.5.6.871-881.1998.
13. Via, L.E.; Lin, P.L.; Ray, S.M.; Carrillo, J.; Allen, S.S.; Seok, Y.E.; Taylor, K.; Klein, E.; Manjunatha, U.; Gonzales, J., et al. Tuberculous granulomas are hypoxic in guinea pigs, rabbits, and nonhuman primates. In *Infection and Immunity*, 2008; Vol. 76, pp 2333-2340.
14. North, R.J.; Ryan, L.; LaCourse, R.; Mogue, T.; Goodrich, M.E. Growth rate of mycobacteria in mice as an unreliable indicator of mycobacterial virulence. In *Infection and Immunity*, American Society for Microbiology: 1999; Vol. 67, pp 5483-5485.
15. Waters, W.R.; Palmer, M.V.; Nonnecke, B.J.; Thacker, T.C.; Scherer, C.F.C.; Estes, D.M.; Hewinson, R.G.; Vordermeier, H.M.; Barnes, S.W.; Federe, G.C., et al. Efficacy and immunogenicity of Mycobacterium bovis Δ RD1 against aerosol M. bovis infection in neonatal calves. In *Vaccine*, 2009; Vol. 27, pp 1201-1209.
16. Palmer, M.V.; Waters, W.R.; Whipple, D.L. Aerosol delivery of virulent Mycobacterium bovis to cattle. Tuberculosis. In *Edinb*, 2003; Vol. 82, pp 275-282.
17. Buddle, B.M.; Skinner, M.A.; Wedlock, D.N.; De Lisle, G.W.; Vordermeier, H.M.; Hewinson, R.G. Cattle as a model for development of vaccines against human tuberculosis. In *Tuberculosis*, Churchill Livingstone: 2005; Vol. 85, pp 19-24.

18. Johnson, L.; Dean, G.; Rhodes, S.; Hewinson, G.; Vordermeier, M.; Wangoo, A. Low-dose *Mycobacterium bovis* infection in cattle results in pathology indistinguishable from that of high-dose infection. In *Tuberculosis*, 2007; Vol. 87.
19. Rodgers, J.D.; Connery, N.L.; McNair, J.; Welsh, M.D.; Skuce, R.A.; Bryson, D.G.; McMurray, D.N.; Pollock, J.M. Experimental exposure of cattle to a precise aerosolised challenge of *Mycobacterium bovis*: A novel model to study bovine tuberculosis. In *Tuberculosis*, 2007; Vol. 87.
20. Larsen, M.H.; Biermann, K.; Jacobs, William R. Laboratory Maintenance of *Mycobacterium tuberculosis* In *Current Protocols in Microbiology*, 2007; Vol. 6.
21. Wangoo, A.; Johnson, L.; Gough, J.; Ackbar, R.; Inglut, S.; Hicks, D.; Spencer, Y.; Hewinson, G.; Vordermeier, M. Advanced granulomatous lesions in *Mycobacterium bovis*-infected cattle are associated with increased expression of type I procollagen, gammadelta (WC1+) T cells and CD 68+ cells. *J Comp Pathol* **2005**, *133*, 223-234, doi:10.1016/j.jcpa.2005.05.001.
22. Waters, W.R.; Palmer, M.V.; Nonnecke, B.J.; Thacker, T.C.; Scherer, C.F.C.; Estes, D.M.; Jacobs, W.R.; Glatman-Freedman, A.; Larsen, M.H. Failure of a *Mycobacterium tuberculosis* Δ RD1 Δ panCD double deletion mutant in a neonatal calf aerosol *M. bovis* challenge model: Comparisons to responses elicited by *M. bovis* bacille Calmette Guerin. In *Vaccine*, 2007; Vol. 25.
23. Alonge, M.; Soyk, S.; Ramakrishnan, S.; Wang, X.; Goodwin, S.; Sedlazeck, F.J.; Lippman, Z.B.; Schatz, M.C. RaGOO: Fast and accurate reference-guided scaffolding of draft genomes. In *Genome Biology*, BioMed Central Ltd.: 2019; Vol. 20.
24. Gurevich, A.; Saveliev, V.; Vyahhi, N.; Tesler, G. QUASt: Quality assessment tool for genome assemblies. In *Bioinformatics*, 2013; Vol. 29, pp 1072-1075.
25. Krzywinski, M.; Schein, J.; Birol, I.I.; Connors, J.; Gascoyne, R.; Horsman, D.; Jones, S.J.; Marra, M.A.; Steven, J.J.; Marra, M.A., et al. Circos: an information aesthetic for comparative genomics. In *Genome Research*, 2009; Vol. 19, pp 1639-1645.
26. Tatusova, T.; Dicuccio, M.; Badretdin, A.; Chetvernin, V.; Nawrocki, E.P.; Zaslavsky, L.; Lomsadze, A.; Pruitt, K.D.; Borodovsky, M.; Ostell, J. NCBI prokaryotic genome annotation pipeline. In *Nucleic Acids Research*, 2016; Vol. 44, pp 6614-6624.
27. Wattam, A.R.; Abraham, D.; Dalay, O.; Disz, T.L.; Driscoll, T.; Gabbard, J.L.; Gillespie, J.J.; Gough, R.; Hix, D.; Kenyon, R., et al. PATRIC, the bacterial bioinformatics database and analysis resource. In *Nucleic Acids Research*, 2014; Vol. 42.
28. Seemann, T. Snippy: Rapid haploid variant calling and core SNP phylogeny. In *GitHub*, 2015.
29. Faksri, K.; Xia, E.; Tan, J.H.; Teo, Y.Y.; Ong, R.T. In silico region of difference (RD) analysis of *Mycobacterium tuberculosis* complex from sequence reads using RD-Analyzer. *BMC Genomics* **2016**, *17*, 847, doi:10.1186/s12864-016-3213-1.
30. Kapopoulou, A.; Lew, J.M.; Cole, S.T. The MycoBrowser portal: A comprehensive and manually annotated resource for mycobacterial genomes. In *Tuberculosis*, 2011; Vol. 91, pp 8-13.
31. Williams, J.T.; Haiderer, E.R.; Coulson, G.B.; Conner, K.N.; Ellsworth, E.; Chen, C.; Alvarez-Cabrera, N.; Li, W.; Jackson, M.; Dick, T., et al. Identification of new MMPL3 inhibitors by untargeted and targeted mutant screens defines MMPL3 domains with differential resistance. In *Antimicrobial Agents and Chemotherapy*, American Society for Microbiology: 2019; Vol. 63.

32. Converse, S.E.; Mougous, J.D.; Leavell, M.D.; Leary, J.A.; Bertozzi, C.R.; Cox, J.S. MmpL8 is required for sulfolipid-1 biosynthesis and Mycobacterium tuberculosis virulence. In *Proc Natl Acad Sci USA*, 2003; Vol. 100, pp 6121- 6126.
33. Domenech, P.; Reed, M.B.; Barry, C.E. Contribution of the Mycobacterium tuberculosis MmpL protein family to virulence and drug resistance. In *Infect Immun*, 2005; pp 3492- 3501.
34. Lamichhane, G.; Tyagi, S.; Bishai, W.R. Designer arrays for defined mutant analysis to detect genes essential for survival of Mycobacterium tuberculosis in mouse lungs. In *Infect Immun*, 2005; Vol. 73, pp 2533- 2540.
35. Seeliger, J.C.; Holsclaw, C.M.; Schelle, M.W.; Botyanszki, Z.; Gilmore, S.A.; Tully, S.E. Elucidation and chemical modulation of sulfolipid-1 biosynthesis in Mycobacterium tuberculosis. In *J Biol Chem*, 2012; Vol. 287, pp 7990- 8000.
36. Degiacomi G, B.J., Pasca MR, De Rossi E, Riccardi G, Chiarelli LR. Promiscuous Targets for Antitubercular Drug Discovery: The Paradigm of DprE1 and MmpL3. In *Applied Sciences.*, 2020; Vol. 10, p 623.
37. Jankute, M.; Alderwick, L.J.; Noack, S.; Veerapen, N.; Nigou, J.; Besra, G.S. Disruption of mycobacterial aftB results in complete loss of terminal $\beta(1 \rightarrow 2)$ arabinofuranose residues of Lipoarabinomannan. In *ACS Chemical Biology*, 2017; Vol. 12.
38. Raad, R.B.; Ménéche, X.; De Sousa-D'Auria, C.; Chami, M.; Salmeron, C.; Tropis, M.; Labarre, C.; Daffé, M.; Houssin, C.; Bayan, N. A deficiency in arabinogalactan biosynthesis affects Corynebacterium glutamicum mycolate outer membrane stability. In *Journal of Bacteriology*, 2010; Vol. 192.
39. Hett, E.C.; Chao, M.C.; Deng, L.L.; Rubin, E.J. A mycobacterial enzyme essential for cell division synergizes with resuscitation-promoting factor. In *PLoS Pathogens*, 2008; Vol. 4.
40. Hett, E.C.; Chao, M.C.; Steyn, A.J.; Fortune, S.M.; Deng, L.L.; Rubin, E.J. A partner for the resuscitation-promoting factors of Mycobacterium tuberculosis. In *Molecular Microbiology*, 2007; Vol. 66.
41. Kana, B.D.; Gordhan, B.G.; Downing, K.J.; Sung, N.; Vostroktunova, G.; Machowski, E.E.; Tsenova, L.; Young, M.; Kaprelyants, A.; Kaplan, G., et al. The resuscitation-promoting factors of Mycobacterium tuberculosis are required for virulence and resuscitation from dormancy but are collectively dispensable for growth in vitro. In *Molecular Microbiology*, 2008; Vol. 67.
42. Kana, B.D.; Mizrahi, V. Resuscitation-promoting factors as lytic enzymes for bacterial growth and signaling. In *FEMS Immunology and Medical Microbiology*, 2010; Vol. 58.
43. Russell-Goldman, E.; Xu, J.; Wang, X.; Chan, J.; Tufariello, J.A.M. A Mycobacterium tuberculosis Rpf double-knockout strain exhibits profound defects in reactivation from chronic tuberculosis and innate immunity phenotypes. In *Infection and Immunity*, 2008; Vol. 76.
44. Cohen-Gonsaud, M.; Barthe, P.; Bagnéris, C.; Henderson, B.; Ward, J.; Roumestand, C.; Keep, N.H. The structure of a resuscitation-promoting factor domain from Mycobacterium tuberculosis shows homology to lysozymes. In *Nature Structural and Molecular Biology*, 2005; Vol. 12.
45. Squeglia, F.; Romano, M.; Ruggiero, A.; Vitagliano, L.; De Simone, A.; Berisio, R. Carbohydrate recognition by RpfB from mycobacterium tuberculosis unveiled by crystallographic and molecular dynamics analyses. In *Biophysical Journal*, 2013; Vol. 104.
46. Cole, S.T.; Brosch, R.; Parkhill, J.; Garnier, T.; Churcher, C.; Harris, D.; Gordon, S.V.; Eiglmeier, K.; Gas, S.; Barry, C.E., et al. Erratum: Deciphering the biology of Mycobacterium tuberculosis from the complete genome sequence (Nature (1998) 393 (537-544)). In *Nature*, 1998; Vol. 396, p 190.

47. Lima, P.; Sidders, B.; Morici, L.; Reader, R.; Senaratne, R.; Casali, N.; Riley, L.W. Enhanced mortality despite control of lung infection in mice aerogenically infected with a *Mycobacterium tuberculosis* mce1 operon mutant. In *Microbes and Infection*, 2007; Vol. 9, pp 1285-1290.
48. Tekaiia, F.; Gordon, S.V.; Garnier, T.; Brosch, R.; Barrell, B.G.; Cole, S.T. Analysis of the proteome of *Mycobacterium tuberculosis* in silico. In *Tuber Lung Dis*, 1999; Vol. 79, pp 329-342.
49. Siméone, R.; Léger, M.; Constant, P.; Malaga, W.; Marrakchi, H.; Daffé, M.; Guilhot, C.; Chalut, C. Delineation of the roles of FadD22, FadD26 and FadD29 in the biosynthesis of phthiocerol dimycocerosates and related compounds in *Mycobacterium tuberculosis*. In *FEBS Journal*, 2010; Vol. 277, pp 2715-2725.
50. Trivedi, O.A.; Arora, P.; Sridharan, V.; Tickoo, R.; Mohanty, D.; Gokhale, R.S. Enzymic activation and transfer of fatty acids as acyl-adenylates in mycobacteria. In *Nature*, 2004; Vol. 428.
51. Gilbert, S.; Hood, L.C.; Seah, S.Y.K. Characterization of an aldolase involved in cholesterol side chain degradation in *Mycobacterium tuberculosis*. In *Journal of Bacteriology*, 2018; Vol. 200.
52. Thomas, S.T.; VanderVen, B.C.; Sherman, D.R.; Russell, D.G.; Sampson, N.S. Pathway profiling in *Mycobacterium tuberculosis*: Elucidation of cholesterol-derived catabolite and enzymes that catalyze its metabolism. In *Journal of Biological Chemistry*, 2011; Vol. 286.
53. Lamont, E.A.; Janagama, H.K.; Ribeiro-lima, J.; Vulchanova, L.; Seth, M.; Yang, M.; Kurmi, K.; Waters, W.R. Circulating *Mycobacterium bovis* Peptides and Host Response Proteins as Biomarkers for Unambiguous Detection of Subclinical Infection. 2014; Vol. 52, pp 536-543.
54. Etienne, G.; Malaga, W.; Laval, F.; Lemassu, A.; Guilhot, C.; Daffé, M. Identification of the polyketide synthase involved in the biosynthesis of the surface-exposed lipooligosaccharides in mycobacteria. In *J Bacteriol*, 2009; Vol. 191, pp 2613-2621.
55. Rousseau, C.; Sirakova, T.; Dubey, V.; Bordat, Y.; Kolattukudy, P.; Gicquel, B.; Jackson, M. Virulence attenuation of two Mas-like polyketide synthase mutants of *Mycobacterium tuberculosis*. In *Microbiology (Reading)*, 2003; Vol. 149, pp 1837-1847.
56. Vaziri, F.; Brosch, R. ESX/Type VII Secretion Systems—An Important Way Out for Mycobacterial Proteins. In *Microbiology Spectrum*, 2019; Vol. 7.
57. Ohol, Y.M.; Goetz, D.H.; Chan, K.; Shiloh, M.U.; Craik, C.S.; Cox, J.S. *Mycobacterium tuberculosis* MycP1 Protease Plays a Dual Role in Regulation of ESX-1 Secretion and Virulence. In *Cell Host and Microbe*, 2010; Vol. 7, pp 210-220.
58. Ganguly, N.; Siddiqui, I.; Sharma, P. Role of *M. tuberculosis* RD-1 region encoded secretory proteins in protective response and virulence. In *Tuberculosis*, 2008; Vol. 88, pp 510-517.
59. Pym, A.S.; Brodin, P.; Brosch, R.; Huerre, M.; Cole, S.T. Loss of RD1 contributed to the attenuation of the live tuberculosis vaccines *Mycobacterium bovis* BCG and *Mycobacterium microti*. In *Molecular Microbiology*, 2002; Vol. 46.